

Impact of $f(\mathfrak{R}, \mathcal{T}^2)$ Theory on Stable Finch-Skea Gravastar Model

M. Sharif¹ *and Saba Naz² †

¹ Department of Mathematics and Statistics, The University of Lahore, 1-KM Defence Road Lahore, Pakistan.

² Department of Mathematics, University of the Punjab, Quaid-e-Azam Campus, Lahore-54590, Pakistan.

Abstract

This paper examines the structure of a gravitationally vacuum star (also known as gravastar) in the background of $f(\mathfrak{R}, \mathcal{T}^2)$ theory. This hypothetical object can be treated as a substitute of a black hole, with three regions: (i) the internal region, (ii) the intrinsic shell and (iii) the outer region. We examine these geometries using Finch-Skea metric for radial metric component along with particular $f(\mathfrak{R}, \mathcal{T}^2)$ model. We determine singularity-free solution for both the inner as well as thin-shell domains. The smooth matching of the interior region with external Schwarzschild spacetime is obtained through Israel matching constraints. Finally, we study various characteristics of gravastar domains including equation of state parameter, proper length, entropy, energy as well as surface redshift. It is found that the compact gravastar structure is a viable alternate to the black hole in the perspective of this gravity.

Keywords: Modified theories; Gravastars; Israel formalism.

PACS: 04.50.Kd; 04.40.Dg.

*msharif.math@pu.edu.pk

†sabanaz1.math@gmail.com

1 Introduction

Cosmic systems incorporating both small as well as large-scale celestial bodies have an impact on the evolution of the universe and provide a platform for astrophysical studies. Different theories have been formulated to comprehend the mechanism and structure of these stellar objects. Einstein formulated general relativity (GR) to investigate the dynamical relationship between space, time, matter, as well as curvature. According to the proposal of Edwin Hubble, all galaxies in the cosmos are moving rapidly farther from us resulting in accelerated cosmic expansion. Various observational evidences have revealed the quick expanding behavior of the cosmos [1]. The cryptic force possessing huge negative pressure referred to as dark energy is assumed to be responsible for this cosmic behavior.

Acceptable cosmic models have been developed by numerous researchers to describe the universe origin, evolution as well as transition through many cosmic epochs. In accordance of big-bang theory, cosmic matter and energy were occupied in a tiny region, also described as singularity with an endless temperature and energy density. Although the big-bang theory is widely accepted, many more fascinating proposals have been put forward by experts to explain the origin and evolution of the cosmos. The universe evolution can also be explained by bounce cycles (continuous expanding as well as contracting behavior) with neither a beginning nor an end and is named as the bounce theory.

Katirci and Kavuk [2] introduced the revolutionary notion of bounce theory to formulate a generalization of GR. Through the contraction of energy-momentum tensor (EMT), they established a particular relation between matter and gravity dubbed as **energy-momentum squared gravity (EMSG)** or $f(\mathfrak{R}, \mathcal{T}^2)$ theory with $\mathcal{T}^2 = T^{\alpha\beta}T_{\alpha\beta}$. This theory is found to be a promising framework for avoiding the big-bang singularity since it has a minimum scale factor and maximum finite density [3]. In this theory, the role of cosmological constant is to resolve singularity by providing a repulsive force. This theory follows the true sequence of cosmic epochs and effectively explains the cosmic behavior. The field equations in this theory incorporate squared and product components of matter variables, which significantly contribute to the investigation of many cosmological scenarios.

Numerous researchers have contributed extensive work regarding this modified theory. Roshan and Shojai [3] solved EMSG field equations with homogeneous perfect matter configuration to compute exact solutions and

determined the possibility of bouncing cosmos at early times. The range of exact solutions for isotropic expanding universe in relation to the early and late-time cosmic evolution was derived by Board and Barrow [4]. The correlation between mass as well as radius of a neutron star was presented in [5]. They found that smaller or larger size of these stars is controlled by the core pressure along with the model parameter of this gravity. Moraes and Sahoo [6] investigated wormhole solutions with non-exotic matter whereas Akarsu et al. [7] studied probable neutron star constraints in the same framework. Bahamonde et al. [8] examined the role of minimal/non-minimal coupled models and concluded that these models well describe the cosmic history and accelerated expansion.

Barbar et al. [41] studied feasible constraints of the bouncing cosmos in this theory and found non-singular universe in the early times. Ranjit et al. [42] used cosmic chronometer as well as Supernovae type-Ia data to study cosmological implications of the solutions for matter density of the proposed EMSG model. Singh et al. [11] used quark matter to explore the structure of celestial bodies. Sharif and Gul [12] discussed various scenarios such as gravitational collapse, Noether symmetry and stability of the Einstein universe in the realm of this theory. We have explored different attributes of gravastar solutions in the presence/absence of electromagnetic field [13]. Recently, Sharif and his collaborators computed solutions through minimal geometric deformation [14] and studied the complexity of charged static sphere as well as uncharged static cylinder in this gravity [15].

The fundamental elements of the galaxies arrayed in a cosmic web are stars which are made of hydrogen and helium. The equilibrium of stars against inward-directed gravitational pull is maintained by burning their fuel. When a star burns all of its fuel in the core, then outer pressure vanishes. Consequently, new compact objects are formed as a final outcome of the gravitational collapse of the star. One of the highly dense objects is an entirely collapsed body regarded as a black hole. In black hole geometry, the event horizon surrounds singularity (known as the place of no return). The pioneering work on stellar structure referred to as gravastar was presented by Mazur and Motolla [16] to study *singularity as well as event horizon* issues. The appealing attribute of this novel compact structure is its *singularity-free* nature. They used the de Sitter (dS) interior to prevent the singularity whereas a very thin layer of baryonic matter disintegrates the outer and inner regions. An equation of state (EoS) governs the characteristics of each domain.

Currently, there is no observational evidence in support of hypothetical gravastar, however, numerous studies indicate the existence as well as detection of gravastar structure in the near future. The criteria for detection of gravastars can be carried out by studying gravastar shadows [18]. To detect gravastar geometries, gravitational lensing (measurement of the overall changing luminosity of companion or nearby stars) was proposed by [19]. In contrast to black holes, we may find a maximum luminosity effect in gravastar structure with a mass equal to that of a black hole. The observation of GW150914 through interferometric LIGO detectors showed ringdown signals hinting towards the possibility of an entity having no event horizon [20]. Furthermore, a current investigation through **First M87 Event Horizon Telescope (EHT)** was made and suggested that captured shadows might be a part of the gravastar geometry [21].

Many astrophysicists are paying close attention to gravastars in an effort to understand more about their structural properties. For particular EoS parameters, Visser and Wiltshire [22] found stable configurations by examining the impact of radial perturbations on gravastar stability. An extension to this work was given by presenting the vacuum energy bounds for inner and outer sectors of gravastar structure [23]. To compute solutions for an extended range of radii as well as masses, Bilić et al. [24] used the dS geometry in the internal domain in place of Born-Infeld phantom spacetime. To study various attributes against shell thickness, an investigation of gravastar solutions incorporating the Kuchowicz metric ansatz was presented by [25]. Ghosh and his collaborators [26] determined gravastar solutions by employing the Karmarkar condition for both the interior as well as shell region.

Das et al. [27] investigated various characteristics of intermediate shell of gravastar in $f(\mathfrak{R}, \mathcal{T})$ gravity and explored some of its features graphically. Shamir and Ahmad [28] inspected gravastar geometry in the context of $f(\mathcal{G}, \mathcal{T})$ theory (*where \mathcal{G} is the Gauss-Bonnet invariant*). Sharif and Waseem [29] investigated gravastar in $f(\mathfrak{R}, \mathcal{T})$ theory using conformal motion and found the object having no singularity. The same authors [30] discussed different features of gravastar geometry through Kuchowicz ansatz. In recent years, several studies [31]-[40] have been devoted to investigate the effects of modified gravity on compact objects, providing important insights into their structural properties and evolution.

The Finch-Skea metric was initially introduced as a correction to the Dourah and Ray [41] metric, which was found unsuitable for describing compact objects. Finch and Skea [42] made modifications to this metric to ac-

commodate relativistic stellar models. However, they further extended the Finch-Skea metric in four dimensions to include anisotropic stellar models [43]-[47]. The significance of the Finch-Skea metric lies in its utility for describing compact stellar configurations in spacetime dimensions equal to or greater than four [48]. These metric potentials have attracted considerable attention from researchers due to their non-singular and viable properties. As a result, they have been extensively employed to study compact stellar structures with diverse matter distributions. For instance, Bhar [49] utilized the Finch-Skea metric potentials and the chaplygin gas EoS to analyze the physical properties of strange stars.

In this paper, we employ the Finch-Skea metric to study gravastar geometry in EMSG theory. We examine the graphical behavior of various attributes of gravastar for a specific model corresponding to the intrinsic shell. The paper is arranged as follows. Section 2 presents basic formalism of $f(\mathfrak{R}, \mathcal{T}^2)$ field equations with Finch-Skea metric component. We discuss three regions of the gravastar geometry with respective EoS in section 3. In section 4, we analyze the obtained solutions graphically corresponding to a specific value of the model parameter. Section 5 presents stability of gravastar structure. The summary of the obtained findings is provided in the last section.

2 Energy-Momentum Squared Theory

In this section, we use perfect matter distribution to develop the field equations of $f(\mathfrak{R}, \mathcal{T}^2)$ theory. The action of this theory is given by [2]

$$I = \frac{1}{2\kappa^2} \int d^4x [f(\mathfrak{R}, T^{\alpha\vartheta}T_{\alpha\vartheta}) + \mathfrak{L}_m] \sqrt{-g}, \quad (1)$$

where \mathfrak{L}_m is the matter Lagrangian density, $\kappa^2 = 1$ denotes the coupling constant and g represents determinant of the metric tensor. The corresponding field equations are

$$\mathfrak{R}_{\alpha\vartheta} f_{\mathfrak{R}} - \frac{1}{2} g_{\alpha\vartheta} f + g_{\alpha\vartheta} \square f_{\mathfrak{R}} - \nabla_{\alpha} \nabla_{\vartheta} f_{\mathfrak{R}} = T_{\alpha\vartheta} - \Theta_{\alpha\vartheta} f_{\mathcal{T}^2}, \quad (2)$$

where $\square = \nabla_{\alpha} \nabla^{\alpha}$, $f \equiv f(\mathfrak{R}, \mathcal{T}^2)$, $f_{\mathcal{T}^2} = \frac{\partial f}{\partial \mathcal{T}^2}$, $f_{\mathfrak{R}} = \frac{\partial f}{\partial \mathfrak{R}}$, and $\Theta_{\alpha\vartheta}$ is

$$\Theta_{\alpha\vartheta} = -4 \frac{\partial^2 \mathfrak{L}_m}{\partial g^{\alpha\vartheta} \partial g^{\beta\eta}} T^{\beta\eta} - 2\mathfrak{L}_m \left(T_{\alpha\vartheta} - \frac{1}{2} g_{\alpha\vartheta} T \right) - T T_{\alpha\vartheta} + 2T_{\alpha}^{\beta} T_{\vartheta\beta}. \quad (3)$$

The EMT describes the relationship between the distribution of matter and energy. Its non-zero components yield physical variables which determine different dynamical characteristics of self-gravitating systems. The non-conserved EMT in this gravity suggests the occurrence of an extra force which governs the non-geodesic particle motion as follows

$$\nabla^\alpha T_{\alpha\vartheta} = \frac{1}{2} [-f_{\mathcal{T}^2} g_{\alpha\vartheta} \nabla^\alpha \mathcal{T}^2 + 2\nabla^\alpha (f_{\mathcal{T}^2} \ominus_{\alpha\vartheta})]. \quad (4)$$

We consider isotropic matter as

$$T_{\alpha\vartheta} = \mathcal{U}_\alpha \mathcal{U}_\vartheta (P + \varrho) - P g_{\alpha\vartheta}, \quad (5)$$

where \mathcal{U}_ϑ symbolizes four-velocity, ϱ and P describe density and pressure of fluid configuration, respectively. Employing Eqs.(3) and (5) with $\mathfrak{L}_m = P$, we have

$$\ominus_{\alpha\vartheta} = -\mathcal{U}_\alpha \mathcal{U}_\vartheta (3P^2 + \varrho^2 + 4P\varrho).$$

The field equations (2) involve product as well as squared matter components, and hence become difficult to solve. Thus, we use a *minimal/non-minimal* model of this gravity. The field equations relating to the non-minimal model becomes complicated, which makes their solutions very challenging. Consequently, we employ a minimally coupled model of the form [2]

$$f(\mathfrak{R}, \mathcal{T}^2) = \mathfrak{R} + \chi \mathcal{T}^2, \quad (6)$$

where χ denotes a model parameter and $\mathcal{T}^2 = \varrho^2 + 3P^2$. This model represents the cosmic evolution and expanding behavior. The inclusion of the component \mathcal{T}^2 results in the extension of $f(\mathfrak{R})$ as well as $f(\mathfrak{R}, T)$ theories beyond GR. Different aspects of several celestial objects have been studied using the functional form (6). It significantly resolves issues related to the universe [50] as well as describes three cosmic epochs, known as **dS-dominated**, **radiation-dominated** as well as **matter-dominated** eras. Employing this relation of $f(\mathfrak{R}, \mathcal{T}^2)$ in Eq.(2), we obtain

$$\mathbb{G}_{\alpha\vartheta} = T_{\alpha\vartheta} + \frac{1}{2} \chi g_{\alpha\vartheta} \mathcal{T}^2 - \chi f_{\mathcal{T}^2} \ominus_{\alpha\vartheta}, \quad (7)$$

where Einstein tensor is denoted by $\mathbb{G}_{\alpha\vartheta}$.

We take a static sphere to investigate the inner geometry of gravastar structure as

$$ds^2 = e^{\sigma(r)} dt^2 - e^{\varpi(r)} dr^2 - r^2(d\theta^2 + \sin^2\theta d\varphi^2). \quad (8)$$

The respective field equations are

$$-e^{-\varpi} r^{-2} + \frac{1}{r^2} + \frac{\varpi' r^{-1}}{e^{\varpi}} = \varrho + \frac{1}{2}\chi\varrho^2 + \frac{3}{2}\chi P^2 + 4\chi\varrho P, \quad (9)$$

$$e^{-\varpi} \left(\frac{1}{r^2} + \frac{\sigma'}{r} \right) - \frac{1}{r^2} = P - \frac{\chi}{2}\varrho^2 - \frac{3}{2}\chi P^2, \quad (10)$$

$$e^{-\varpi} \left(\frac{\sigma'^2}{4} + \frac{\sigma'}{2r} - \frac{\varpi'}{2r} + \frac{\sigma''}{2} - \frac{\sigma'\varpi'}{4} \right) = P - \frac{\chi}{2}\varrho^2 - \frac{3}{2}\chi P^2, \quad (11)$$

where the radial derivative is denoted by prime. The radial metric component $e^{\varpi(r)}$ is considered to be of the form proposed by Finch-Skea and is given as [51]

$$e^{\varpi(r)} = 1 + \aleph r^2, \quad (12)$$

where \aleph is an arbitrary constant. Plugging Eq.(20) in (9)-(11), we have

$$\aleph + 2\mathfrak{F} = \frac{\aleph}{\mathfrak{F}} \left[\varrho + \frac{\chi(\varrho^2 + 3P^2 + \varrho P)}{2} \right], \quad (13)$$

$$\aleph - \frac{\sigma'}{r} = \frac{\aleph}{\mathfrak{F}} \left(P - \frac{\chi}{2}\varrho^2 - \frac{3}{2}\chi P^2 \right), \quad (14)$$

$$\mathfrak{F} - \frac{\sigma'}{2r} - \frac{1}{2} \left[\sigma'' + \frac{\sigma'^2}{2} - \sigma' r \mathfrak{F} \right] = \frac{\aleph}{\mathfrak{F}} \left(P - \frac{\chi}{2}\varrho^2 - \frac{3}{2}\chi P^2 \right), \quad (15)$$

with $\mathfrak{F} = \frac{\aleph}{1+\aleph r^2}$. The non-conservation equation (4) gives

$$\frac{dP}{dr} + \sigma' \left(\frac{P + \varrho}{2} \right) + \mathfrak{B}^* = 0, \quad (16)$$

where \mathfrak{B}^* determines the impact of $f(\aleph, \mathcal{T}^2)$ theory as

$$\mathfrak{B}^* = \left[\sigma' (4P\varrho + 3P^2 + \varrho^2) + (3PP' + \varrho\varrho') \right] \frac{\chi}{2}.$$

3 Structure of Gravastar

A thin shell of ultra-relativistic fluid covers the internal region of gravastar, while the Schwarzschild metric describes the exterior vacuum region. The following three domains provide a complete picture of the gravastar structure.

$$(A) \text{ Interior domain } (J_1) \ (0 \leq r < \mathcal{K}_1 = \mathcal{K}) \quad \implies \quad \varrho = -P.$$

$$(B) \text{ Intrinsic shell } (J_2) \ (\mathcal{K}_1 \leq r \leq \mathcal{K}_2) \quad \implies \quad P = \varrho.$$

$$(C) \text{ Exterior domain } (J_3) \ (r > \mathcal{K}_2 = \mathcal{K} + \epsilon) \quad \implies \quad \varrho = 0 = P.$$

The small thickness of the intermediate shell is described by ϵ .

3.1 The Internal Geometry

We adopt the EoS, $P = \mathcal{W}\varrho$, where \mathcal{W} is the EoS parameter, as proposed by Mazur and Mottola [16]. The inner region of gravastar structure is described by $P = -\varrho$ (for $\mathcal{W} = -1$). Consequently, a large amount of negative pressure produced in core is applied on the intrinsic shell of the spherical object and counterbalances the outward gravitational force. Equation (16) alongwith dark energy EoS yields $\varrho = \varrho_c$ (constant) which gives

$$P = -\varrho = -\varrho_c. \tag{17}$$

This equation reads that matter variables (*pressure as well as energy density*) are constants throughout the interior region. The other obtained solution from Eq.(16) is $(1 + 2\chi P) = 0$ which gives $P = \frac{-1}{2\chi}$. This relation suggests that only when the model parameter has a positive value, we obtain negative pressure in the current setup which is necessarily required in the inner core to prevent collapse. This negative pressure and inward-acting force coming from shell counteract each other. In order to accurately reflect this notion, our discussion specifically considers the positive values of the model parameter. We determine the radial metric component as

$$e^{\varpi} = e^{(\mathcal{F} - 4\mathcal{G}\varrho_c + C_1)}, \tag{18}$$

where $\mathcal{F} = \frac{8r^2}{2}$, $\mathcal{G} = (\frac{r^2}{2} + \frac{ar^4}{4})(2\pi + \chi)$ and C_1 denotes an integration constant.

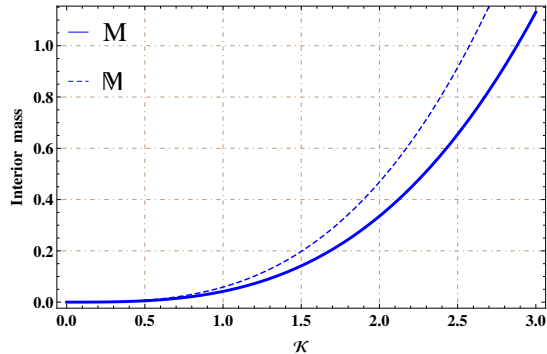


Figure 1: Graphical trend of gravitational mass corresponding to regular energy density (Thick) and effective energy density (Dotted) for $\chi = 2.5$.

The mass of celestial body for regular energy density is defined by $M = \int 4\pi \varrho r^2 dr$, whereas in realm of $f(\mathfrak{R}, \mathcal{T}^2)$, the effective energy density leads to

$$\mathbb{M}(\mathcal{K}) = \frac{\varrho_c(4\pi + \chi\varrho_c)\mathcal{K}^3}{3}. \quad (19)$$

Figure 1 shows the graphs of the gravitational mass corresponding to regular density denoted by M whereas \mathbb{M} describes the gravitational mass corresponding to effective energy density. It is obvious that thin-shell mass increases exponentially in relation to thickness of the shell. This is the expected behavior (for example, same outcomes were found for gravastars, employing conformal motion in EMSG gravity [17]).

3.2 The Intermediate Shell

The correlation, $P = \varrho$, is followed by the intermediate shell region (occupying stiff fluid). The stiff matter configuration proposed by Zel'dovich [52] was used by researchers to have some interesting results regarding cosmic and astrophysical issues [53]-[57]. In present scenario, exact solution of density is not possible. Thus, the interpolating function of density is determined by incorporating stiff matter EoS whose graphical behavior is observed in Figure 2. The plot of density shows the positive linear profile.

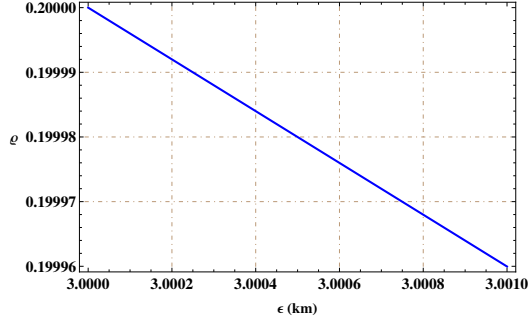


Figure 2: Trend of energy density against ϵ (shell thickness) for $\chi = 2.5$.

3.3 The External Region and Israel Matching Constraint

To comprehend the unknown factors, it is essential to explore certain physical constraints that are useful in investigating the inner region of celestial bodies. By establishing a direct correlation between the inner and outer regions of stellar objects, we can effectively analyze the exact composition and behavior of heavenly structures. In this pursuit, physicists often rely on different spacetimes to examine the outer geometry of stellar objects under various conditions. In the context of general relativity (GR), the Schwarzschild spacetime is employed to study non-charged objects, whereas the Reissner-Nordstrom metric is used for charged objects. In recent study conducted by Kalita and Mukhopaddhyay [58], they investigated a modified asymptotically flat vacuum solution, which is considered the best candidate for external spacetime to facilitate smooth matching in modified theories of gravity.

The modified spherically symmetric vacuum solution suitable for representing the external region of stellar objects is given as follows

$$ds_+^2 = S dt^2 - \frac{\mathfrak{P}}{S} dr^2 - r^2 d\theta^2 - r^2 \sin^2 \theta d\phi^2, \quad (20)$$

where

$$S = 1 - \frac{2}{r} - \frac{B(B-6)}{2r^2} + \frac{B^2(13B-66)}{20r^3} - \frac{B^3(31B-156)}{48r^4} + \frac{3B^4(11B-57)}{56r^5} - \frac{B^5(67B-360)}{128r^6} + \dots, \quad \mathfrak{P} = \frac{16r^4}{(B+2r)^4}.$$

Here \mathbf{B} is a real constant. It is mentioned here that two boundaries complete the structure of gravastar, one connects the inner region to the intermediate shell, whereas the other connects the intermediate shell to the exterior space-time. At these boundaries, the continuity of metric potentials define physically well behaved system. It is very crucial to determine the constraints necessary for the smooth joining of both inner as well as outer domains. Israel formalism plays vital role in attaining these constraints which make possible the smooth joining of these domains. The metric coefficients must be continuous over the hypersurface ($r = \mathcal{K}$), but the continuity between their differentials may not hold.

The Lanczos equation is employed to compute the stress-energy tensor as follows

$$S_{\xi}^{\zeta} = (\delta_{\xi}^{\zeta} \pi_l^l - \mathfrak{S}_{\xi}^{\zeta}) \frac{1}{8\pi}, \quad (21)$$

where $\mathfrak{S}_{\zeta\xi} = \mathcal{G}_{\zeta\xi}^+ - \mathcal{G}_{\zeta\xi}^-$ exhibits that the extrinsic curvature is discontinuous. Here, + sign symbolizes the outer region of the gravastar whereas - sign corresponds to the inner region. The components of extrinsic curvature at the hypersurface are described by

$$\mathcal{G}_{\zeta\xi}^{\pm} = -n_{\gamma}^{\pm} \left[\frac{\partial^2 x^{\gamma}}{\partial \zeta^{\zeta} \partial \xi^{\xi}} + \Upsilon_{\lambda\delta}^{\gamma} \left(\frac{\partial x^{\lambda}}{\partial \zeta^{\zeta}} \right) \left(\frac{\partial x^{\delta}}{\partial \xi^{\xi}} \right) \right], \quad (22)$$

where thin-shell coordinates are represented by ζ^{ξ} and the unit normal (n_{γ}^{\pm}) is defined as

$$n_{\gamma}^{\pm} = \pm \left| g^{\lambda\delta} \frac{\partial \Pi}{\partial x^{\lambda}} \frac{\partial \Pi}{\partial x^{\delta}} \right|^{-\frac{1}{2}} \frac{\partial \Pi}{\partial x^{\gamma}}, \quad n_{\gamma} n^{\gamma} = 1. \quad (23)$$

The isotropic EMT is given as $S_{\xi}^{\zeta} = \text{diag}(\mathcal{Y}, -\mathcal{Z}, -\mathcal{Z})$, where the surface energy density and surface pressure are represented by \mathcal{Y} and \mathcal{Z} , respectively and are given by Lanczos equations as

$$\mathcal{Y} = -\frac{1}{4\pi\mathcal{K}} \left[\sqrt{\mathcal{S}} - \sqrt{e^{(\mathcal{F}-4\mathcal{G}\varrho_c)}} \right], \quad (24)$$

$$\mathcal{Z} = \frac{1}{8\pi\mathcal{K}} \left[\frac{\mathcal{S}'}{\sqrt{\mathcal{S}}} - \frac{e^{(\mathcal{F}-4\mathcal{G}\varrho_c)} (1 + \mathcal{K}(\mathcal{F}' - 4\mathcal{G}'\varrho_c))}{\sqrt{e^{(\mathcal{F}-4\mathcal{G}\varrho_0)}}} \right]. \quad (25)$$

The surface energy density is used to calculate mass of the intermediate shell and is given as

$$m_{shell} = 4\pi\mathcal{K}^2\mathcal{Y} = \mathcal{K} \left[\sqrt{e^{(\mathcal{F}-4\mathcal{G}\varrho_c)}} - \sqrt{\mathcal{S}} \right]. \quad (26)$$

Consequently, the total mass of the gravastar structure is

$$\mathcal{M} = \left[e^{(\mathcal{F}-4\mathcal{G}\varrho_c)} \right]^{\frac{1}{2}} m_{shell} + \frac{(4\pi + \chi\varrho_c)2\varrho_c\mathcal{K}^3}{3} - \frac{m_{shell}^2}{2\mathcal{K}}. \quad (27)$$

4 Some Physical Features Gravastar Intrinsic-Shell

This section investigates significant gravastar features (EoS parameter, length, energy, entropy as well as surface redshift versus thin-shell thickness).

4.1 Equation of State Parameter

At $r = \mathcal{K}$, we employ Eqs.(24) and (25) to compute EoS parameter for the thin-shell region of gravastar geometry as

$$\mathcal{W} = \frac{\mathcal{Z}}{\mathcal{Y}} = \frac{\frac{1}{8\pi\mathcal{K}} \left[\frac{1-\frac{\mathcal{M}}{\mathcal{K}}}{\sqrt{\frac{\mathcal{K}-2\mathcal{M}}{\mathcal{K}}}} - \frac{1+\aleph\mathcal{K}^2}{(1+\aleph\mathcal{K}^2)^{\frac{3}{2}}} \right]}{-\frac{1}{4\pi\mathcal{K}} \left[\sqrt{1-\frac{2\mathcal{M}}{\mathcal{K}}} - \sqrt{\frac{1}{1+\aleph\mathcal{K}^2}} \right]}. \quad (28)$$

The validity of various stellar models is well described by different values of the EoS parameter. For instance, $\mathcal{W} = 0$ indicates flat surfaces comprising of non-relativistic fluid, $\mathcal{W} = \frac{-1}{3}$ is for curved surfaces, $\mathcal{W} = -1$ for dark energy, $\mathcal{W} < -1$ represents phantom energy and $\mathcal{W} \geq -1$ describes non-phantom regime. In present scenario, interior domain occupies dark energy so we take $\mathcal{W} = -1$ showing significance of gravastar structure.

4.2 Length of thin-Shell

The distance from the internal region boundary to the intermediate shell determines the length of the gravastar structure. It is expressed by

$$L = \int_{\mathcal{K}}^{\mathcal{K}+\epsilon} \sqrt{e^{\overline{\omega}}} dr. \quad (29)$$

Differentiating this with respect to r , it follows that

$$L'(r) = (1 + \aleph r^2)^{\frac{1}{2}} \Big|_{\mathcal{K}}^{\mathcal{K}+\epsilon}. \quad (30)$$

The behavior of length is examined graphically in Figure 3 which indicates that thin-shell length increases with shell thickness.

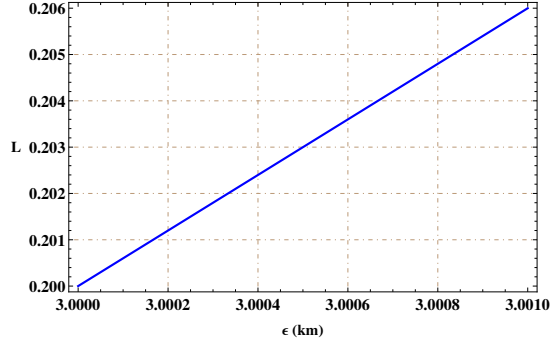


Figure 3: Plot of proper length versus thickness ϵ for $\chi = 2.5$.

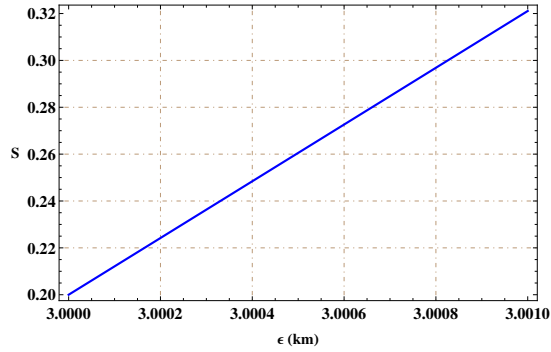


Figure 4: Entropy corresponding to thickness of intrinsic shell for $\chi = 2.5$.

4.3 Entropy of the Intermediate Shell

The degree of disorder in a particular region of a structure is referred to as entropy. The inner domain entropy is found to be zero in literature [16]. The disorderness within intermediate shell is described by

$$S = 4\pi \int_{\mathcal{K}}^{\mathcal{K}+\epsilon} \mathbf{s}(\mathbf{r}) \sqrt{e^{\varpi}} r^2 dr, \quad (31)$$

where $\mathbf{s}(\mathbf{r})$ is the entropy density. The plot of entropy (Figure 4) illustrates the continuous increasing profile of randomness of the shell region. This indicates that the dark source terms of $f(\mathfrak{R}, \mathcal{T}^2)$ gravity enhance the randomness of the celestial object.

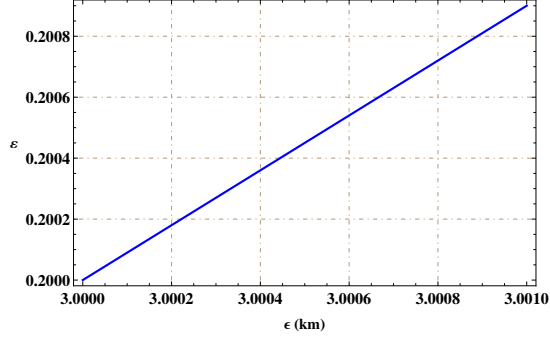


Figure 5: Energy profile against thickness of the shell for $\chi = 2.5$.

4.4 Energy of Intrinsic-Shell

The internal domain of the gravastar geometry occupies dark energy providing anti-attractive force whereas energy of the shell region is provided by

$$\varepsilon = \int_{\mathcal{K}}^{\mathcal{K}+\epsilon} \frac{1}{2} \rho r^2 dr. \quad (32)$$

Figure 5 shows the increasing profile of the thin-shell energy versus ϵ .

4.5 Surface Redshift of Intrinsic Shell

The surface redshift is considered to be an important information source for the stability and detection of gravastars in the structural investigation of gravastars. The redshift parameter is always less than 2 for isotropic matter distribution [59]. It is given as

$$z = \frac{1}{\sqrt{|g_{rr}|}} - 1. \quad (33)$$

Figure 6 shows that the value of redshift parameter remains in its required bound within the shell of gravastar geometry.

5 Stability

Here, we investigate system equilibrium to assess the stability of the resulting solution through adiabatic index. Equation (16) involves two forces, i.e.,

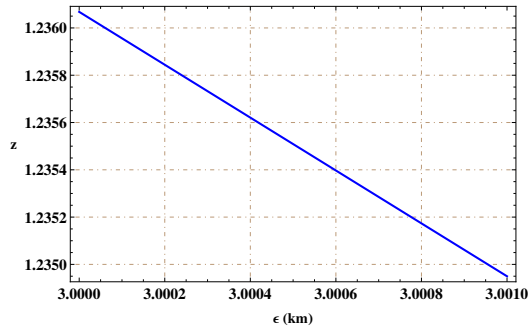


Figure 6: Behavior of surface redshift for $\chi = 2.5$.

hydrodynamical $F_{\mathbf{h}}$ and gravitational force $F_{\mathbf{g}}$ given by

$$F_{\mathbf{h}} = \frac{dP}{dr} + 3\chi P P',$$

$$F_{\mathbf{g}} = \sigma' \left(\frac{\varrho + P}{2} \right) + \chi \left(\frac{3P^2 + \varrho^2 + 4P\varrho}{2} \right) \sigma' + \chi \varrho \varrho'.$$

The above forces describe equilibrium state by counterbalancing the impact of each other. These forces include squared as well as product matter components and combined effect of these forces turn out to be zero. To discuss the stability of celestial bodies, we utilize the adiabatic index. The pioneering proposal of Chandrasekhar helps in checking the dynamical stability of celestial body through small adiabatic perturbations. Chandrasekhar found that the adiabatic index must not exceed the value $4/3$ for the relativistic system to be stable and is described as

$$\Gamma = \frac{P + \varrho}{P} \frac{dP}{d\varrho}.$$

For the inner domain with EoS $P = -\varrho$, we obtain $\Gamma = 0$ and for the thin-shell domain with EoS $P = \varrho$, it follows that $\Gamma = 2$. This shows that the internal sector is unstable but intermediate shell sector is stable.

6 Conclusions

In this paper, we have computed solutions of gravastar geometry by employing the Finch-Skea metric in the perspective of $f(\mathfrak{R}, \mathcal{T}^2)$ gravity. The behavior of Finch-Skea metric potential is regular and non-singular throughout

gravastar structure. In order to better understand different characteristics of the gravastar structure, we have developed solutions for each domain of the gravastar by using minimal coupling model $f(\mathfrak{R}, \mathcal{T}^2) = \mathfrak{R} + \chi\mathcal{T}^2$. The metric components as well as matter density in the internal region of the gravastar are evaluated. The constant energy density is obtained throughout the gravastar structure by employing $\rho = -P$ in the conservation equation. The exterior domain exerts pressure on thin-shell and singularity formation is avoided by maintaining balance between outward directed pressure and gravitational force acting inward. Consequently, the singularity is prevented at the core of the gravastar. We have observed that gravitational mass is positive throughout the inner region but zero at the core.

We have also explored attributes of gravastar structure such as matter density, EoS parameter, length, entropy, energy and surface redshift against intrinsic shell thickness. The major findings are summarized as follows.

- The finite positive behavior of density is found versus shell thickness. As the thickness of a thin-shell increases, so does the density (Figure 2). Thus the shell outer boundary is denser than its inner boundary.
- The gravastar length against intermediate shell shows an increasing profile (Figure 3). In $f(\mathfrak{R}, \mathcal{T}^2)$, the value of length is observed as 0.206 which is less than that of 2.6217008 found in $f(\mathfrak{R}, \mathcal{T})$ theory [60].
- The entropy of gravastar structure is linearly connected to thickness of thin-shell. We have found higher entropy with increasing thickness (Figure 4). The shell region entropy is 0.32 for $\epsilon = 3.0010km$ in the present scenario while its value is found to be 2.1630 in $f(\mathfrak{R}, \mathcal{T})$ gravity [60]. It is notable that disorderness of the considered system in realm of $f(\mathfrak{R}, \mathcal{T}^2)$ theory is less than that of $f(\mathfrak{R}, \mathcal{T})$ gravity.
- We have found linear behavior of the energy of gravastar thin-shell versus shell thickness (Figure 5). We have computed that energy of the shell region is 0.2008 for $\epsilon = 0.30010km$ while in other scenario is 0.3538 [60]. Thus, the shell energy is decreased for this choice of EMSG model.
- The surface red shift provides the acceptable behavior as it lies in the required limit.

- Finally, we have checked the hydrostatic equilibrium to analyze stability of the system. We have also discussed the adiabatic index to study the stability of gravastar. It is found that the stellar model meets the specified range of stability criteria.

We would like to mention here that various studies on gravastar structure in the realm of modified theories of gravity have been carried out [61]-[63]. The discussed attributes, i.e., length, entropy and energy present proportional behavior. In comparison to our obtained outcomes, we have found consistent behavior with those given in the literature [61]-[63]. These features demonstrate physical viability as well as stability of the considered structure in the context of $f(\mathcal{R}, \mathcal{T}^2)$ theory. Thus the construction of a gravastar-like compact object with Finch-Skea ansatz is realistic in this modified theory.

Data Availability Statement: This manuscript does not contain any new data.

References

- [1] Pietrobon, D., Balbi, A. and Marinucci, D.: Phys. Rev. D **74**(2006)043524; Astieer, P. et al.: Astron. Astrophys. **447**(2016)31.
- [2] Katirci, N. and Kavuk, M.: Eur. Phys. J. Plus **129**(2014)163.
- [3] Roshan, M. and Shojai, F.: Phys. Rev. D **94**(2016)044002.
- [4] Board, C.V.R. and Barrow, J.D.: Phys. Rev. D **96**(2017)123517.
- [5] Nari, N. and Roshan, M.: Phys. Rev. D **98**(2018)024031.
- [6] Moraes, P.H.R.S. and Sahoo, P.K.: Phys. Rev. D **97**(2018)2.
- [7] Akarsu, O. et al.: Phys. Rev. D **97**(2018)124017.
- [8] Bahamonde, S., Marciu, M. and Rudra, P.: Phys. Rev. D **100**(2019)083511.
- [9] Barbar, A.H., Awad, A.M. and AlFiky, M.T.: Phys. Rev. D **101**(2020)044058.
- [10] Ranjit, C. Rudra, P. and Kundu, S.: Ann. Phys. **428**(2021)168432.

- [11] Singh, K.N. et al: Phys. Dark Universe **31**(2021)100774.
- [12] Sharif, M. and Gul, M.Z.: Phys. Scr. **96**(2020)025002; Int. J. Mod. Phys. A **36**(2021)2150004; Adv. Astron. **2021**(2021)6663502; Eur. Phys. J. Plus **136**(2021)503; Chin. J. Phys. **71**(2021)365; Universe **07**(2021)154; Phys. Scr. **96**(2021)105001.
- [13] Sharif, M. and Naz, S.: Universe **8**(2022)142; Eur. Phys. J. Plus **137**(2022)421; Int. J. Mod. Phys. D **31**(2022)2240008; Mod. Phys. Lett. A **37**(2022)2250065; *ibid.* 2250125.
- [14] Sharif, M. and Iltaf, S.: Phys. Scr. **97**(2022)075002; Chin. J. Phys. **79**(2022)173.
- [15] Sharif, M. and Anjum, A.: Eur. Phys. J. Plus **137**(2022)602; Gen. Relativ. Gravit **54**(2022)111.
- [16] Mazur, P. and Mottola, E.: Proc. Natl. Acad. Sci. **101**(2004)9545.
- [17] Sharif, M. and Saeed, M.: Chin. J. Phys. **77**(2022)583.
- [18] Sakai, N. et al.: Phys. Rev. D **90**(2014)104013.
- [19] Kubo, T. and Sakai, N.: Phys. Rev. D **93**(2016)084051.
- [20] Cardoso, V. et al.: Phys. Rev. Lett. **116**(2016)171101; *ibid.* **117**(2016)089902 .
- [21] Akiyama, K. et al.: Astrophys. J. Lett. **875**(2019)1.
- [22] Visser, M. and Wiltshire, D.L.: Class. Quantum Grav. **21**(2004)1135.
- [23] Carter, B.M.N.: Class. Quantum Grav. **22**(2005)4551.
- [24] Bilić, N., Tupper, G.B. and Viollier, R.D.: J. Cosmol. Astropart. Phys. **02**(2006)013.
- [25] Ghosh, S. et al.: Res. Phys. **14**(2019)102473.
- [26] Ghosh, S. et al.: Ann. Phys. **411**(2019)167968.
- [27] Das, A. et al.: Phys. Rev. D **95**(2017)124011.

- [28] Shamir, M. and Ahmad, M.: Phys. Rev. D **97**(2018)104031.
- [29] Sharif, M. and Waseem, A.: Astrophys. Space Sci. **364**(2019)189.
- [30] Sharif, M. and Waseem, A.: Int. J. Mod. Phys. D **28**(2019)1950033; ibid. 2040005.
- [31] Cruz-Dombriz, A. and Saez-Gomez, D.: Entropy **14**(2012)1717.
- [32] Staykov, K.V.: J. Cosmol. Astropar. Phys. **10**(2014)006.
- [33] Yazadjiev, S.S. et al.: J. Cosmol. Astropar. Phys. **06**(2014)003.
- [34] Yazadjiev, S.S., Doneva, D.D. and Kokkotas, K.D.: Phys. Rev. D **91**(2015)084018; ibid. **92**(2015)064015; ibid. **96**(2017)064002; Eur. Phys. J. C **78**(2018)818.
- [35] Capozziello, S. et al.: Phys. Rev. D **93**(2016)023501.
- [36] Doneva, D.D. et al.: Phys. Rev. D **98**(2018)104039.
- [37] Olmo, G.J., Rubiera-Garcia, D. and Wojnar, A.: Phys. Rept. **876**(2020)1.
- [38] Feola, P. et al.: Phys. Rev. D **101**(2020)044037.
- [39] Odintsov, S.D. and Oikonomou, V.K.: Phys. Rev. D **107**(2023)104039.
- [40] Oikonomou, V.K.: Class. Quantum Grav. **40**(2023)085005; Monthly Notices Royal Astronom. Soc. **520**(2023)2934.
- [41] Dourah, H.L. and Ray, R.: Class. Quantum Grav. **4**(1987)1691.
- [42] Finch, M.R. and Skea, J.E.F.: Class. Quantum Grav. **6**(1989)467.
- [43] Kalam, M. et al.: Int. J. Theor. Phys. **52**(2013)3319.
- [44] Banerjee, A. et al.: Gen. Relativ. Gravit. **45**(2013)717.
- [45] Hansraj, S. et al.: Int. J. Mod. Phys. D **15**(2006)1311.
- [46] Hansraj, S. and Maharaj, S.D.: Int. J. Mod. Phys. D **15**(2006)1311.

- [47] Sharma, R., Das, S. and Thirukkanesh, S.: *Astrophys. Space Sci.* **362**(2017)12.
- [48] Paul, B.C. and Dey, S.: *Astrophys. Space Sci.* **363**(2018)220.
- [49] Bhar, P.: *Astrophys. Space Sci.* **359**(2015)41.
- [50] Akarsu, O. Katirci, N., and Kumar, S.: *Phys. Rev. D* **97**(2018)024011.
- [51] Finch, M.R. and Skea, J.E.F.: *Class. Quantum Grav.* **4**(1989)467.
- [52] Zel'dovich, Y.B.: *Mon. Not. R. Astron. Soc.* **160**(1972)1.
- [53] Carr, B.J.: *Astrophys. J.* **201**(1975)1.
- [54] Wesson, P.S.: *J. Math. Phys.* **19**(1978)2283.
- [55] Madsen, M.S. et al.: *Phys. Rev. D* **46**(1992)1399.
- [56] Braje, T.M. and Romani, R.W.: *Astrophys. J.* **580**(2002)1043.
- [57] Linares, L.P., Malheiro, M. and Ray, S.: *Int. J. Mod. Phys. D* **13**(2004)1355.
- [58] Kalita, S. and Mukhopadhyay, B.: *Eur. Phys. J. C* **79**(2019)877.
- [59] Buchdahl, H.A.: *Phys. Rev.* **116**(1959)1027; Barraco, D.E. and Hamity, V.H.: *Phys. Rev. D* **65**(2002)124028.
- [60] Majeeda, K., Abbas, G. and Siddiqa, A.: *New Astron.* **95**(2022)101802.
- [61] Bhar, P.: *Astrophys. Space Sci.* **354**(2014)457; *Int. J. Geom. Methods Mod. Phys.* **18**(2021)2150112.
- [62] Das, A. et al.: *Phys. Rev. D* **95**(2017)124011; Das, A. et al.: *Nucl. Phys. B* **954**(2020)114986.
- [63] Bhar, P and Rej, P.: *Eur. Phys. J. C* **81**(2021)763.